

# We are IntechOpen, the world's leading publisher of Open Access books Built by scientists, for scientists

6,900

Open access books available

185,000

International authors and editors

200M

Downloads

Our authors are among the

154

Countries delivered to

TOP 1%

most cited scientists

12.2%

Contributors from top 500 universities



WEB OF SCIENCE™

Selection of our books indexed in the Book Citation Index  
in Web of Science™ Core Collection (BKCI)

Interested in publishing with us?  
Contact [book.department@intechopen.com](mailto:book.department@intechopen.com)

Numbers displayed above are based on latest data collected.  
For more information visit [www.intechopen.com](http://www.intechopen.com)



# Design of a Neural Controller for Walking of a 5-Link Planar Biped Robot via Optimization

Nasser Sadati<sup>1,2</sup>, Guy A. Dumont<sup>1</sup>, and Kaveh Akbari Hamed<sup>2</sup>

<sup>1</sup>*Electrical and Computer Engineering Department,  
The University of British Columbia, Vancouver,*

<sup>2</sup>*Electrical Engineering Department, Sharif University of Technology, Tehran,*

<sup>1</sup>*BC Canada*

<sup>2</sup>*Iran*

## 1. Introduction

Underactuation, impulsive nature of the impact with the environment, the existence of feet structure and the large number of degrees of freedom are the basic problems in control of the biped robots. Underactuation is naturally associated with dexterity [1]. For example, headstands are considered dexterous. In this case, the contact point between the body and the ground is acting as a pivot without actuation. The nature of the impact between the lower limbs of the biped walker and the environment makes the dynamic of the system to be impulsive. The foot-ground impact is one of the main difficulties one has to face in design of robust control laws for biped walkers [2]. Unlike robotic manipulators, biped robots are always free to detach from the walking surface and this leads to various types of motions [2]. Finally, the existence of many degrees of freedom in the mechanism of biped robots makes the coordination of the links difficult. According to these facts, designing practical controller for biped robots remains to be a challenging problem [3]. Also, these features make applying traditional stability margins difficult.

In fully actuated biped walkers where the stance foot remains flat on the ground during single support phase, well known algorithms such as the Zero Moment Point (ZMP) principle guarantees the stability of the biped robot [4]. The ZMP is defined as the point on the ground where the net moment generated from ground reaction forces has zero moment about two axes that lie in the plane of ground. Takanishi [5], Shin [6], Hirai [7] and Dasgupta [8] have proposed methods of walking patterns synthesis based on ZMP. In this kind of stability, as long as the ZMP lies strictly inside the support polygon of the foot, then the desired trajectories are dynamically feasible. If the ZMP lies on the edge of the support polygon, then the trajectories may not be dynamically feasible. The Foot Rotation Indicator (FRI) [9] is a more general form of the ZMP. FRI is the point on the ground where the net ground reaction force would have to act to keep the foot stationary. In this kind of stability, if FRI is within the convex hull of the stance foot, the robot is possible to walk and it does not roll over the toe or the heel. This kind of walking is named as fully actuated walking. If FRI is out of the foot projection on the ground, the stance foot rotates about the toe or the heel. This is also named as underactuated walking. For bipeds with point feet [10] and

Source: Human-Robot Interaction, Book edited by: Daisuke Chugo,  
ISBN 978-953-307-051-3, pp. 288, February 2010, INTECH, Croatia, downloaded from SCIYO.COM

Passive Dynamic walkers (PDW) [11] with curved feet in single support phase, the ZMP heuristic is not applicable. Westervelt in [12] has used the Hybrid Zero Dynamics (HZD) [13], [14] and Poincaré mapping method [15]-[18] for stability of RABBIT using underactuated phase. The controller proposed in this approach is organized around the hybrid zero dynamics so that the stability analysis of the closed loop system may be reduced to a one dimensional Poincaré mapping problem. HZD involves the judicious choice of a set of holonomic constraints that were imposed on the robot via feedback control [19]. Extracting the eigenvalues of Poincaré return map is commonly used for analyzing PDW robots. But using of eigenvalues of Poincaré return maps assumes periodicity and is valid only for small deviation from limit cycle [20].

The ZMP criterion has become a very powerful tool for trajectory generation in walking of biped robots. However, it needs a stiff joint control of the prerecorded trajectories and this leads to poor robustness in unknown rough terrain [20] while humans and animals show marvelous robustness in walking on irregular terrains. It is well known in biology that there are Central Pattern Generators (CPG) in spinal cord coupling with musculoskeletal system [21]-[23]. The CPG and the feedback networks can coordinate the body links of the vertebrates during locomotion. There are several mathematical models which have been proposed for a CPG. Among them, Matsuoka's model [24]-[26] has been studied more. In this model, a CPG is modeled by a Neural Oscillator (NO) consisting of two mutually inhibiting neurons. Each neuron in this model is represented by a nonlinear differential equation. This model has been used by Taga [22], [23] and Miyakoshi [27] in biped robots. Kimura [28], [29] has used this model at the hip joints of quadruped robots.

The robot studied in this chapter is a 5-link planar biped walker in the sagittal plane with point feet. The model for such robot is hybrid [30] and it consists of single support phase and a discrete map to model the frictionless impact and the instantaneous double support phase. In this chapter, the goal is to coordinate and control the body links of the robot by CPG and feedback network. The outputs of CPG are the target angles in the joint space, where P controllers at joints have been used as servo controllers. For tuning the parameters of the CPG network, the control problem of the biped walker has been defined as an optimization problem. It has been shown that such a control system can produce a stable limit cycle (i.e. stride). The structure of this chapter is as follows. Section 2 models the walking motion consisting of single support phase and impact model. Section 3 describes the CPG model and tuning of its parameters. In Section 4, a new feedback network is proposed. In Section 5, for tuning the weights of the CPG network, the problem of walking control of the biped robot is defined as an optimization problem. Also the structure of the Genetic algorithm for solving this problem is described. Section 6 includes simulation results in MATLAB environment. Finally, Section 7 contains some concluding remarks.

## 2. Robot model

The overall motion of the biped involves continuous phases separated by abrupt changes resulting from impact of the lower limbs with the ground. In single support phase and double support phase, the biped is a mechanical system that is subject to unilateral constraints [31]-[33]. In this section, the biped robot has been assumed as a planar robot consisting of  $n$  rigid links with revolute and parallel actuated joints to form a tree structure. In the single support phase, the mechanical system consists of  $n + 2$  DOF, where  $n - 1$

DOF associated with joint coordinates which are actuated, two DOF associated with horizontal and vertical displacements of the robot in the sagittal plane which are unactuated, and one DOF associated with orientation of the robot in sagittal plane which is also unactuated. With these assumptions, the generalized position vector of the system ( $q_e$ ) can be split in two subsets  $q$  and  $r$ . It can be expressed as

$$q_e := (q^T, r^T)^T, \quad (1)$$

where  $q := (q_0, q_1, \dots, q_{n-1})^T$  encapsulates the joint coordinates and  $q_0$  which is the unactuated DOF between the stance leg and the ground. Also  $r := (x, y)^T \in \mathbb{R}^2$  is the Cartesian coordinates of the stance leg end.

### A. Single support phase

Figure 1 depicts the single support phase and configuration variables of a 5-link biped robot ( $n = 5$ ). In the single support phase, second order dynamical model immediately follows from Lagrange's equation and the principle of virtual work [34]-[36]

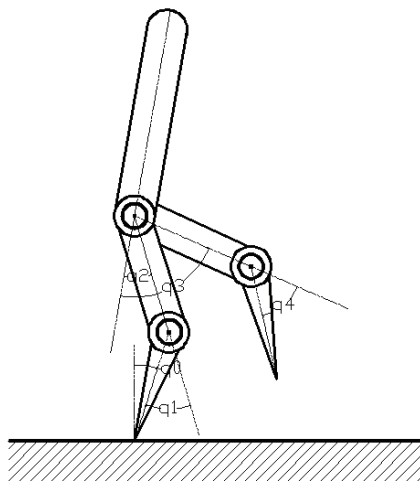


Fig. 1. Single support phase and the configuration variables.

$$M_e(q_e)\ddot{q}_e + H_e(q_e, \dot{q}_e) + G_e(q_e) = B_e u - B_e F_e(q_e, \dot{q}_e) + J_e^{st}(q_e)^T F^{ext, st}, \quad (2)$$

where  $M_e(q_e) \in \mathbb{R}^{(n+2) \times (n+2)}$  is the symmetric and positive definite inertia matrix,  $H_e(q_e, \dot{q}_e) \in \mathbb{R}^{n+2}$  includes centrifugal and Coriolis terms and  $G_e(q_e) \in \mathbb{R}^{n+2}$  is the vector containing gravity terms. Also  $u := (u_1, u_2, \dots, u_{n-1})^T \in \mathbb{R}^{n-1}$  includes the joint torques applied at the joints of the robot,  $B_e \in \mathbb{R}^{(n+2) \times (n-1)}$  is the input matrix,  $F_e(q_e, \dot{q}_e) \in \mathbb{R}^{n-1}$  includes the joint frictions modeled by viscous and static friction terms,  $J_e^{st}(q_e) := \partial r^{st} / \partial q_e \in \mathbb{R}^{2 \times (n+2)}$  is the Jacobian at the stance leg end. Also  $F^{ext, st} := (F_x^{ext, st}, F_y^{ext, st})^T \in \mathbb{R}^2$  is the ground reaction force at the stance leg end. With setting  $q_e := (q^T, r^T)^T$  in (2), the dynamic equation of the mechanical system can be rewritten as the following form

$$\begin{bmatrix} \frac{M_{11}(q)}{M_{12}(q)^T} & \frac{M_{12}(q)}{m I_2} \end{bmatrix} \begin{bmatrix} \ddot{q} \\ \ddot{r} \end{bmatrix} + \begin{bmatrix} H_{e1}(q_e, \dot{q}_e) \\ H_{e2}(q_e, \dot{q}_e) \end{bmatrix} + \begin{bmatrix} G_{e1}(q_e) \\ G_{e2}(q_e) \end{bmatrix} = \begin{bmatrix} 0 \\ u \\ 0_{2 \times 1} \end{bmatrix} - \begin{bmatrix} 0 \\ F(q, \dot{q}) \\ 0_{2 \times 1} \end{bmatrix} + J_e^{st}(q_e)^T \begin{bmatrix} F_x^{ext, st} \\ F_y^{ext, st} \end{bmatrix}, \quad (3)$$

where  $m$  is the total mass of the robot. If we assume that the Cartesian coordinates have been attached to the stance leg end and the stance leg end is stationary (i.e. in contact with the ground and not slipping), these assumptions (i.e.  $r = 0$ ,  $\dot{r} = 0$ ,  $\ddot{r} = 0$ ) will allow one to solve for the ground reaction force as explicit functions of  $(q, \dot{q}, u)$  [37], [38]. Also, the dynamic equation in (3) will be reduced with this assumptions and this will lead to a lower dimensional mechanical model which describes the single support phase if the stance leg end is stationary as follows

$$\begin{aligned} M(q)\ddot{q} + H(q, \dot{q}) + G(q) &= \begin{bmatrix} 0 \\ u \end{bmatrix} - \begin{bmatrix} 0 \\ F(q, \dot{q}) \end{bmatrix} \\ F^{ext, st} &= \Psi(q, \dot{q}, u), \end{aligned} \quad (4)$$

where  $M(q) = M_{11}(q)$  and  $\Psi(\cdot) : TQ \times \mathbb{R}^{n-1} \rightarrow \mathbb{R}^2$  is a nonlinear mapping of  $(q, \dot{q}, u)$ . Also  $TQ := \{x := (q^T, \dot{q}^T)^T \mid q \in Q, \dot{q} \in \mathbb{R}^n\}$  is the state space of the reduced model where  $Q$  is a simply connected, open subset of  $[-\pi, \pi]^n$ . Note that  $q_0$  is an unactuated DOF in (4) (i.e. without actuation) and hence  $\dim u < \dim q$ . It can be shown that

$$\Psi(q, \dot{q}, u) = \begin{bmatrix} \sum_{i=1}^n m_i \ddot{x}_i \\ \sum_{i=1}^n m_i (\ddot{y}_i + g) \end{bmatrix} = \begin{bmatrix} m \ddot{x}_{cm} \\ m(\ddot{y}_{cm} + g) \end{bmatrix}, \quad (5)$$

where  $r_i := (x_i, y_i)^T$  and  $r_{cm} := (x_{cm}, y_{cm})^T$  are the coordinate of the mass center of link  $i$  and the mass center of the robot, respectively,  $m_i$  is the mass of the link  $i$  and  $g$  is the gravitational acceleration. With assumption  $x_{cm} = f_1(q)$  and  $y_{cm} = f_2(q)$ , we have

$$\ddot{r}_{cm}(q, \dot{q}, \ddot{q}) = \begin{bmatrix} \partial f_1 / \partial q \\ \partial f_2 / \partial q \end{bmatrix} \ddot{q} + \begin{bmatrix} \dot{q}^T (\partial^2 f_1 / \partial q^2) \dot{q} \\ \dot{q}^T (\partial^2 f_2 / \partial q^2) \dot{q} \end{bmatrix}. \quad (6)$$

With setting  $\ddot{q} = M(q)^{-1}(0, \bar{u}^T)^T - M(q)^{-1}(H(q, \dot{q}) + G(q))$  where  $\bar{u} := u - F(q, \dot{q})$  from equation (4) in equation (6) and using equation (5), we have

$$\begin{aligned} \Psi(q, \dot{q}, u) &= m J^c(q) M^{-1}(q) \begin{bmatrix} 0 \\ u \end{bmatrix} - m J^c(q) M^{-1}(q) \begin{bmatrix} 0 \\ F(q, \dot{q}) \end{bmatrix} - m J^c(q) M^{-1}(q) H(q, \dot{q}) \\ &\quad - m J^c(q) M^{-1}(q) G(q) + m \begin{bmatrix} \dot{q}^T H_1(q) \dot{q} \\ \dot{q}^T H_2(q) \dot{q} \end{bmatrix} + \begin{bmatrix} 0 \\ mg \end{bmatrix}, \end{aligned} \quad (7)$$

where  $J^c(q) := \partial r_{cm} / \partial q = \begin{bmatrix} \partial f_1 / \partial q \\ \partial f_2 / \partial q \end{bmatrix} \in \mathbb{R}^{2 \times n}$  is the Jacobian matrix at the center of mass, also  $H_1(q) := \partial^2 f_1 / \partial q^2 \in \mathbb{R}^{n \times n}$  and  $H_2(q) := \partial^2 f_2 / \partial q^2 \in \mathbb{R}^{n \times n}$ . The validity of the reduced model in (4) is dependent on two following conditions

$$\begin{aligned} i) \quad & \ddot{y}_{cm} + g > 0 \\ ii) \quad & |\ddot{x}_{cm}| < \mu |\ddot{y}_{cm} + g|, \end{aligned} \quad (8)$$

where  $\mu$  is the static friction coefficient between the stance leg end and the ground. The first condition in (8) is to ensure that the stance leg end is contact with the walking surface and the second condition is to ensure that the slipping does not occur at the stance leg end [39]. The dynamic equation of (4) in the state-variable is expressed as  $\dot{x} = f(x) + g(x)u$  where  $x := (q^T, \dot{q}^T)^T \in TQ$  is the state vector. If we assume that  $x_1 := q$  and  $x_2 := \dot{q}$ , we get  $x = (x_1^T, x_2^T)^T$  and

$$\begin{aligned} f(x) &= \begin{bmatrix} x_2 \\ -M^{-1}(x_1) \left( H(x_1, x_2) + G(x_1) + \begin{pmatrix} 0 \\ F(x_1, x_2) \end{pmatrix} \right) \end{bmatrix} \\ g(x) &= \begin{bmatrix} 0_{n \times n-1} \\ M^{-1}(x_1) \begin{pmatrix} 0_{1 \times n-1} \\ I_{n-1} \end{pmatrix} \end{bmatrix}. \end{aligned} \quad (9)$$

## B. Frictionless impact model

In this section, following assumptions are done for modeling the impact [40]:

- A1. the impact is frictionless (i.e.  $F(q, \dot{q}) = 0$ ). The main reason for this assumption is the problem arising of the introducing of dry friction [2];
- A2. the impact is instantaneous;
- A3. the reaction forces due to the impact at impact point can be modeled as impulses;
- A4. the actuators at joints are not impulsive;
- A5. the impulsive forces due to the impact may result in instantaneous change in the velocities, but there is no instantaneous change in the positions;
- A6. impact results in no slipping and no rebound of the swing leg; and
- A7. stance foot lifts from the ground without interaction.

With these assumptions, impact equation can be expressed by the following equation

$$M_e(q_e) \dot{q}_e(t^+) - M_e(q_e) \dot{q}_e(t^-) = J_e^{sw}(q_e)^T \delta F^{ext, sw}, \quad (10)$$

where  $\delta F^{ext, sw} := \int_{t^-}^{t^+} F^{ext, sw}(\tau) d\tau$  is the impulsive force at impact point and

$J_e^{sw}(q_e) := \partial r^{sw} / \partial q_e \in \mathbb{R}^{2 \times (n+2)}$  is the Jacobian matrix at the swing leg end. The assumption A6 implies that impact is plastic. Hence, impact equation becomes

$$\begin{aligned} M_e(q_e)\dot{q}_e(t^+) - J_e^{sw}(q_e)^T \delta F^{ext,sw} &= M_e(q_e)\dot{q}_e(t^-) \\ J_e^{sw}(q_e)\dot{q}_e(t^+) &= 0. \end{aligned} \quad (11)$$

This equation is solvable if the coefficient matrix has full rank. The determinant of the coefficient matrix is equal to  $\det M_e(q_e) \times \det(J_e^{sw}(q_e)M_e(q_e)^{-1}J_e^{sw}(q_e)^T)$  and it can be shown that the coefficient matrix has full rank iff the robot is not in singular position. The solution of the equation in (11) can be given by the following equation

$$\begin{bmatrix} \dot{q}_e(t^+) \\ \delta F^{ext,sw} \end{bmatrix} = \Lambda(q_e) \begin{bmatrix} M_e(q_e)\dot{q}_e(t^-) \\ 0 \end{bmatrix}, \quad (12)$$

where

$$\Lambda(q_e) := \begin{bmatrix} M_e(q_e) & -J_e^{sw}(q_e)^T \\ J_e^{sw}(q_e) & 0 \end{bmatrix}^{-1}, \quad (13)$$

and also  $q_e(t^-) := (q(t^-)^T, 0, 0)^T$  and  $q_e(t^+) := (q(t^+)^T, 0, 0)^T$ . The map from  $\dot{q}_e(t^-)$  to  $\dot{q}_e(t^+)$  without relabeling is

$$\begin{aligned} \dot{q}_e(t^+) &= \Lambda_{11}(q_e)M_e(q_e)\dot{q}_e(t^-) \\ \delta F^{ext,sw} &= \Lambda_{21}(q_e)M_e(q_e)\dot{q}_e(t^-). \end{aligned} \quad (14)$$

After solving these equations, it is necessary to change the coordinates since the former swing leg must now become the stance leg. Switching due to the transfer of pivot to the point of contact is done by relabeling matrix [39], [40]  $R \in \mathbb{R}^{n \times n}$ . Hence, we have

$$\begin{aligned} q(t^+) &= Rq(t^-) \\ \dot{q}(t^+) &= R \begin{bmatrix} I_n & 0_{n \times 2} \end{bmatrix} \Lambda_{11}(q_e)M_e(q_e)\dot{q}_e(t^-). \end{aligned} \quad (15)$$

The final result is an expression for  $x^+$  in terms of  $x^-$ , which is written as [39]-[41]

$$x^+ = \Delta(x^-). \quad (16)$$

In equation (16),  $\Delta(\cdot) : S \rightarrow TQ$  is the impact mapping where  $S := \{(q, \dot{q}) \in TQ \mid y^{sw}(q) = 0\}$  is the set of points of the state-space where the swing leg touches the ground.  $x^+ := (q(t^+)^T, \dot{q}(t^+)^T)^T$  and  $x^- := (q(t^-)^T, \dot{q}(t^-)^T)^T$  are the state vector of the system after impact and the state vector of the system before impact, respectively. Also, we have

$$\Delta(x^-) := \begin{bmatrix} Rx_1(t^-) \\ \Sigma(x_1(t^-))x_2(t^-) \end{bmatrix}, \quad (17)$$



where  $\Sigma(.) : Q \rightarrow \mathbb{R}^{n \times n}$  by  $\Sigma(x_1(t^-)) := R \begin{bmatrix} I_n & 0_{n \times 2} \end{bmatrix} \Lambda_{11}(q_e) M_e(q_e) \begin{bmatrix} I_n \\ 0_{2 \times n} \end{bmatrix}$ . The ground reaction force due to the impact can be shown as the following form

$$\delta F^{ext,sw} = \Gamma(x_1(t^-))x_2(t^-), \quad (18)$$

where  $\Gamma(.) : Q \rightarrow \mathbb{R}^{2 \times n}$  by  $\Gamma(x_1(t^-)) := \Lambda_{21}(q_e) M_e(q_e) \begin{bmatrix} I_n \\ 0_{2 \times n} \end{bmatrix}$ . The validity of the results of equation (17) depends on two following conditions

$$\begin{aligned} i) \quad & \Theta(x_1(t^-))x_2(t^-) > 0 \\ ii) \quad & \mu \left| \Gamma_2(x_1(t^-))x_2(t^-) \right| - \left| \Gamma_1(x_1(t^-))x_2(t^-) \right| > 0, \end{aligned} \quad (19)$$

where  $\Theta(x_1(t^-)) := J_y^{sw}(Rx_1(t^-))\Sigma(x_1(t^-)) \in \mathbb{R}^{1 \times n}$  and  $J_y^{sw}(q) := \partial y^{sw} / \partial q \in \mathbb{R}^{1 \times n}$ . The first condition is to ensure that the swing foot lifts from the ground at  $t^+$ . The second condition is to ensure that the impact results in no slipping [39]. The valid results are used to re-initialize the model for next step. Furthermore, the double support phase has been assumed to be instantaneous. If we define

$$\Omega := \{x = (x_1^T, x_2^T)^T \in S \mid \Theta(x_1)x_2 > 0, \mu \left| \Gamma_2(x_1)x_2 \right| - \left| \Gamma_1(x_1)x_2 \right| > 0\}, \quad (20)$$

the hybrid model of the mechanical system can be given by

$$\begin{aligned} \dot{x} &= f(x) + g(x)u & x^- \notin S \\ x^+ &= \Delta(x^-) & x^- \in \Omega, \end{aligned} \quad (21)$$

where  $x^-(t) := \lim_{\tau \rightarrow t^-} x(\tau)$ . For  $x^- \in S - \Omega$ , this model is not valid. Also the validity conditions in (8) can not be expressed only as a function of  $x$  and they can be expressed as a function of  $(x, u)$ .

### 3. Control system

Neural control of human locomotion is not yet fully understood, but there are many evidences suggesting that the main control of vertebrates is done by neural circuits called central pattern generators (CPG) in spinal cord which have been coupled with musculoskeletal system. These central pattern generators with reflexes can produce rhythmic movements such as walking, running and swimming.

#### A. Central pattern generator model

There are several mathematical models proposed for CPG. In this section, neural oscillator model proposed by Matsuoka has been used [24], [25]. In this model, each neural oscillator consists of two mutually inhibiting neurons (i.e. extensor neuron and flexor neuron). Each neuron is represented by the following nonlinear differential equations



$$\begin{aligned}
\tau \dot{u}_{\{e,f\}i} &= -u_{\{e,f\}i} + w_{fe} y_{\{f,e\}i} - \beta v_{\{e,f\}i} + u_0 + Feed_{\{e,f\}i} + \sum_{j=1}^n w_{\{e,f\}ij} y_{\{e,f\}j} \\
\tau' \dot{v}_{\{e,f\}i} &= -v_{\{e,f\}i} + y_{\{e,f\}i} \\
y_{\{e,f\}i} &= \max(0, u_{\{e,f\}i}),
\end{aligned} \tag{22}$$

where suffixes  $f$  and  $e$  mean flexor muscle and extensor muscle, respectively. Also suffix  $i$  means the  $i$ th oscillator.  $u_i$  is the inner state of  $i$ th neuron,  $y_i$  is the output of the  $i$ th neuron,  $v_i$  is a variable which represents the degree of self-inhibition effect of the  $i$ th neuron,  $u_0$  is an external input from brain with a constant rate and  $Feed_i$  is a feedback signal from the mechanical system which can be an angular position or an angular velocity. Moreover,  $\tau$  and  $\tau'$  are the time constants associated with  $u_i$  and  $v_i$ , respectively,  $\beta$  is a constant representing the degree of the self-inhibition influence on the inner state and  $w_{ij}$  is a connecting weight between the  $i$ th and  $j$ th neurons. Finally, the output of the neural oscillator is a linear combination of the extensor neuron inner state and the flexor neuron inner state

$$y_{NO,i} = -p_e u_{e,i} + p_f u_{f,i}. \tag{23}$$

The positive or negative value of  $y_{NO,i}$  corresponds to activity of flexor or extensor muscle, respectively. The output of the neural oscillator can be used as a reference trajectory, joint torque and phase. In this chapter, it is used as a reference trajectory at joints. The studied robot (see Fig. 1) has four actuated joints (i.e. hip and knee joints of the legs). We assume that one neural oscillator has been used for generating reference trajectories at each of the actuated joints.

## B. Tuning of the CPG parameters

The walking period is a very important factor since it much influences stability, maximum speed and energy consumption. The walking mechanism has its own natural frequency determined mainly by the length of the links of the legs. It appears that humans exploit the natural frequencies of their arms, swinging pendulums at comfortable frequencies equal to the natural frequencies [26]. Human arms can be thought of as masses connected by springs, whose frequency response makes the energy and the control required to move the arm vary with frequency [26]. Humans certainly learn to exploit the dynamics of their limbs for rhythmic tasks [42], [43]. Robotic examples of this idea include open-loop stable systems where the dynamics are exploited giving systems which require little or no active control for stable operation (e.g. PDW [11]). At the resonant frequency, the control need only inject a small amount of energy to maintain the vibration of the mass of the arm segment on the spring of the muscles and tendons. Extracting and using the natural frequency of the links of the robots is a desirable property of the robot controllers. According to these facts, we match the endogenous frequency of each neural oscillator with the resonant frequency of the corresponding link. On the other hand, when swinging or supporting motions of the legs are closer to the free motion, there will not be any additional acceleration and deceleration and the motion will be effective [44]. When no input is applied to the CPG, the frequency of it is called endogenous frequency. Endogenous frequency of the CPG is mainly determined

by  $\tau$  and  $\tau'$ . In this section, we change the value of  $\tau$  with constant value of  $\tau/\tau'$ . In this case, the endogenous frequency of CPG is proportional to  $1/\tau$ . It was pointed out that the proper value of the  $\tau/\tau'$  for stable oscillation is within  $[0.1,0.5]$  [42]. After tuning the time constants of the CPG, other parameters of CPG can be tuned by using the necessary conditions for free oscillation. These necessary conditions for free oscillation can be written as the following form [24], [25]

i)  $\beta > -w_{fe} - 1$   
ii)  $w_{fe} < -(1 + \tau/\tau')$   
iii)  $u_0 > 0.$

(24)

Table I specifies the lengths, masses and inertias of each link of the robot studied in this chapter [3]. By these data and extracting and using resonant frequencies of the links, we match the endogenous frequency of the CPG with the resonant frequency of each link. In this case,  $\tau$  is designed at 0.13 (s) and  $\tau' = 1.53\tau = 0.2$  (s) for all of the neural oscillators. According to conditions in (24), we tune  $\beta$  and  $w_{fe}$  to 2 and -2, respectively. Also  $u_0$  is equal to 5. The amplitude of the output signal of the CPG is approximately proportional to  $u_0$ ,  $p_e$  and  $p_f$ . The output parameters of the CPGs (i.e.  $p_e$  and  $p_f$  of oscillators at the knee and the hip joints) can be determined by the amplitude of the desired walking algorithm. Table II specifies the designed values of the output parameters of the oscillators at the knee and the hip joints of the robot.

	mass (kg)	length (m)	inertia (kgm <sup>2</sup> )
Torso	12.00	0.625	1.33
Femur	6.80	0.40	0.47
Tibia	3.20	0.40	0.20

Table I. The parameters of the robot

	knee	hip
$p_f$	0.11	0.15
$p_e$	0.01	0.02

Table II. The output parameters of the cpg

4. Feedback network

It is well known in biology that the CPG network with feedback signals from body can coordinate the members of the body, but there is not yet a suitable biological model for feedback network. The control loop used in this section is shown in the Fig. 2 where  $\tilde{\theta} := (q_1, q_2, q_3, q_4)^T$  encapsulates the actuated joint coordinates and there is not any feedback signal from the unactuated DOF (i.e.  $q_0$ ). The feedback network in this control loop is for autonomous adaptation of the CPG network. In other hand, by using feedback network, the

CPG network (i.e. the higher level of the control system) can correct its outputs (i.e. reference trajectories) in various conditions of the robot.

In animals, the stretch reflexes act as feedback loop [44]. In this section, the feedback signals to the CPG neurons of the hip joints are the tonic stretch reflex as follows [22], [23]

$$\begin{aligned} Feed_{e,h} &= k_{tsr,h}(\theta_{hip} - \theta_{0,hip}) \\ Feed_{f,h} &= -k_{tsr,h}(\theta_{hip} - \theta_{0,hip}), \end{aligned} \quad (25)$$

where  $k_{tsr,h}$  is a constant value and also  $\theta_{0,hip}$  is the neutral point of this feedback loop at hip joints. We tune the  $k_{tsr,h}$  and  $\theta_{0,hip}$  to 1 and 0 (rad), respectively.

One of important factors in control of walking is the coordination of the knee and the hip joints in each leg. For tuning the phase difference between the oscillators of the knee and the hip joints in each leg, we propose the following feedback structure which is applied only at oscillators of the knee joints

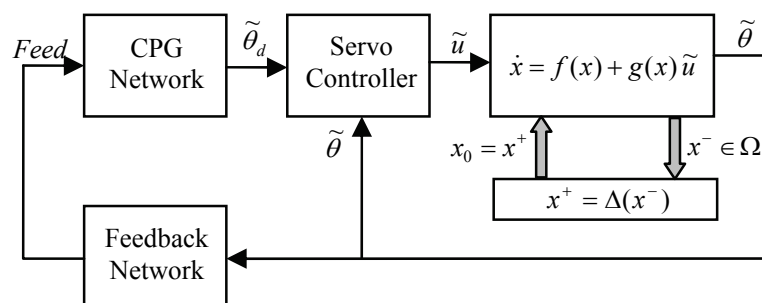


Fig. 2. The control loop used for the biped walker.

$$\begin{aligned} Feed_{e,k} &= k_{tsr,k}(\theta_{knee} - \theta_{0,knee})u(-\dot{\theta}_{hip}) + k_f(\theta_{hip} - \bar{\theta}_{0,hip})u(\dot{\theta}_{hip}) \\ Feed_{f,k} &= -k_{tsr,k}(\theta_{knee} - \theta_{0,knee})u(-\dot{\theta}_{hip}) - k_f(\theta_{hip} - \bar{\theta}_{0,hip})u(\dot{\theta}_{hip}), \end{aligned} \quad (26)$$

where  $k_{tsr,h}$  and  $k_f$  are constant values,  $\theta_{0,knee}$  is the neutral point of the tonic stretch reflex signal at knee joints and  $u(\cdot)$  is a unit step function. The first terms of feedback signals in (26) are the tonic stretch reflex terms. These terms are active in stance phase (i.e.  $\dot{\theta}_{hip} < 0$ ). With these terms, we force the mechanical system to fix the stance knee at a certain angular position (i.e.  $\theta_{0,knee}$ ) during the single support phase like the knee joints of the human being. We call  $\theta_{0,knee}$  as the bias of the stance knee. In this section, we tune  $k_{tsr,h}$  and  $\theta_{0,knee}$  to 10 and 0.1 (rad), respectively. The second terms in (26) are active in swinging phase (i.e.  $\dot{\theta}_{hip} > 0$ ). These terms force the knee oscillator to increase its output at the beginning of swinging phase (i.e.  $\theta_{hip} < \bar{\theta}_{0,hip}$ ). Also these terms force the knee oscillator to decrease its output at the end of swinging phase (i.e.  $\theta_{hip} > \bar{\theta}_{0,hip}$ ). We tune  $k_f$  and  $\bar{\theta}_{0,hip}$  to 4 and 0 (rad), respectively.

## 5. Tuning of the weights in the CPG network

The coordination and the phase difference among the links of the biped robot in the discussed control loop are done by the synaptic weights of connections in the CPG network. There are two kinds of connections in the CPG network. One of them is the connections among the flexor neurons and the other one is the connections among the extensor neurons.

The neural oscillators in the CPG network can be relabeled as shown in the Fig. 3. According to this relabeling law,

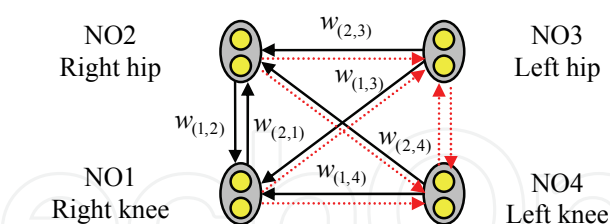


Fig. 3. The CPG network and the synaptic connections.

NO1, NO2, NO3 and NO4 correspond to the right knee, the right hip, the left hip and the left knee neural oscillators, respectively. We show the weight matrix among the flexor and extensor neurons by  $W_f$  and  $W_e$ , respectively. According to the symmetry between the right leg and the left leg, these matrixes can be written as the following form

$$W_{\{f,e\}} = \begin{bmatrix} 0 & w_{\{f,e\},(1,2)} & w_{\{f,e\},(1,3)} & w_{\{f,e\},(1,4)} \\ w_{\{f,e\},(2,1)} & 0 & w_{\{f,e\},(2,3)} & w_{\{f,e\},(2,4)} \\ w_{\{f,e\},(2,4)} & w_{\{f,e\},(2,3)} & 0 & w_{\{f,e\},(2,1)} \\ w_{\{f,e\},(1,4)} & w_{\{f,e\},(1,3)} & w_{\{f,e\},(1,2)} & 0 \end{bmatrix}. \quad (27)$$

This symmetry can be given by the following equations

$$\begin{aligned} w_{\{f,e\},(i,j)} &= w_{\{f,e\},(5-i,5-j)} & ; i, j &= 1, \dots, 4 \\ w_{\{f,e\},(i,i)} &= 0 & ; i &= 1, \dots, 4. \end{aligned} \quad (28)$$

In this chapter, we assume  $W_f = W_e$ . With this assumption and the symmetry between legs, there are six unknown weights which should be determined (bold lines in Fig. 3). For tuning the unknown weights of the CPG network, we should use a tool of the concept of stability for the biped robots. But the concept of stability and stability margin for biped robots is difficult to precisely define, especially for underactuated biped robots with point feet. Since the discussed robot in this chapter has point feet, the ZMP heuristic is not applicable for trajectory generation and verification of the dynamic feasibility of trajectories during execution. In addition, extracting the eigenvalues magnitude of the Poincaré return map may be sufficient for analyzing periodic bipedal walking but they are not sufficient for analyzing nonperiodic motions such as when walking over discontinuous rough terrain. Also, large disruptions from a limit cycle, such as when being pushed, cannot be analyzed using this technique. Some researchers [45] have suggested that angular momentum about the Center of Mass (CoM) should be minimized throughout a motion. As studied in [20], minimizing the angular momentum about the CoM is neither necessary nor sufficient condition for stable walking. According to these facts, for tuning the weights of the CPG network, we define the control problem of the underactuated biped walking as an optimization problem. By finding the optimal solution of the optimization problem, the unknown weights are determined. The total cost function of the optimization problem in this chapter is defined as a summation of sub cost functions and it can be given by

$$J(X) := a_1 J_1(X) + a_2 J_2(X) + a_3 J_3(X), \quad (29)$$

where

$$X := (w_{(1,2)}, w_{(1,3)}, w_{(1,3)}, w_{(2,1)}, w_{(2,3)}, w_{(2,4)})^T \quad (30)$$

and  $X \in [-0.5, 0.5]^6$ . Also  $a_i; i = 1, 2, 3$  are the positive weights. The first sub cost function in (29) can be defined as a criterion of the difference between the distance travelled by the robot in the sagittal plane and the desired distance

$$J_1(X) := \frac{1}{D_m} \sum_{T_1 + \dots + T_i \leq t_f} sl(T_i), \quad (31)$$

where  $sl(T_i)$  is the step length of the  $i$ th step,  $T_i$  is the time duration of the  $i$ th step and  $D_m$  is an upper bound of the traveled distance. Also,  $t_f$  is the duration of the simulation. This sub cost function is a good criterion of the stability.

The second sub cost function in (29) can be defined as the least value of the normalized height of the CoM of the mechanical system during simulation and it can be given by

$$J_2(X) := \min_{t \in [0, t_f]} \frac{y_{cm}(t)}{y_{cm, \max}}, \quad (32)$$

where  $y_{cm, \max}$  is the value of the height of the CoM where the vector  $q$  is equal to zero. Since the biped should maintain an erect posture during locomotion, this sub cost function is defined as a criterion of the erect body posture.

The regulation of the rate change of the angular momentum about the CoM is not a good indicator of whether a biped will fall but the reserve in angular momentum that can be utilized to help recover from push or other disturbance is important. We use the rate change of the angular momentum about the CoM for defining the third sub cost function. With

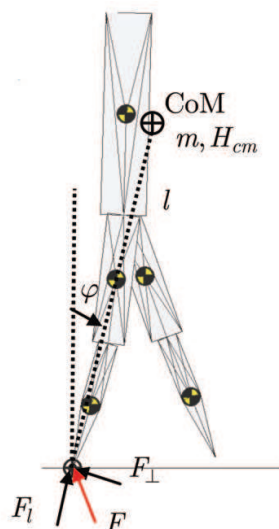


Fig. 4. The virtual inverted pendulum.

setting  $x_{cm} = l \sin \varphi$  and  $y_{cm} = l \cos \varphi$  in equation (5) where  $l$  is the distance from the stance leg end to the CoM and  $\varphi$  is the angle from the stance leg end to the CoM with vertical being zero (see Fig. 4), the equation (5) becomes

$$\begin{aligned} ml^2\ddot{\varphi} + 2ml\dot{\varphi} - mgl \sin \varphi &= -lF_{\perp} \\ m\ddot{l} - ml\dot{\varphi}^2 + mg \cos \varphi &= F_l, \end{aligned} \quad (33)$$

where  $F_l := F_x^{ext,st} \sin \varphi + F_y^{ext,st} \cos \varphi$  and  $F_{\perp} := -F_x^{ext,st} \cos \varphi + F_y^{ext,st} \sin \varphi$ . Also, the total momentum about the stance leg end consists of the angular momentum of the CoM rotating the stance foot plus the angular momentum about the CoM

$$H_{tot} = ml^2\dot{\varphi} + H_{cm}, \quad (34)$$

where  $H_{tot}$  and  $H_{cm}$  are the angular momentums about the stance leg end and CoM, respectively. Also the net angular momentum rate change is equal to  $\dot{H}_{tot} = mgx_{cm} = mgl \sin \varphi$  [3], [20]. With differentiating of equation (34) and setting  $\dot{H}_{tot} = mgl \sin \varphi$  in it and comparing with equation (33), it can be shown that

$$\dot{H}_{cm} = lF_{\perp}. \quad (35)$$

Hence, the third sub cost function is defined as following

$$J_3(X) := \frac{1}{1 + \int_0^{t_f} |\dot{H}_{cm}(t)|^2 dt} = \frac{1}{1 + \int_0^{t_f} |l(t)F_{\perp}(t)|^2 dt}. \quad (36)$$

In this chapter,  $a_1 = 4$ ,  $a_2 = 1$  and  $a_3 = 1$  and the control problem of the biped walking is defined as the optimal solution of the following optimization problem

$$\max_X J(X). \quad (37)$$

By using Genetic algorithm, the optimal solution can be determined. Genetic algorithm is one of the evolutionary algorithms based on the natural selection. In this section, the size of each generation in this algorithm is equal to 400, and at the end of each generation, 50% of chromosomes are preserved and the others are discarded. The roulette strategy is employed for selection and 100 selections are done by this strategy. With applying one-point crossover, 200 new chromosomes are produced. The mutation is done for all of the chromosomes with the probability of 10% except the elite chromosome which has the most fitness. Also, each parameter is expressed in 8 bits.

## 6. Simulation results

In this section, the simulation of a 5 link planar biped robot is done in MATLAB environment. Table I specifies the lengths, masses and inertias of each link of the robot. This is the model of RABBIT [3]. RABBIT has 50:1 gear reducers between its motors and links. In this biped robot, the joint friction is modeled by viscous and static friction terms as



described by  $F(q,\dot{q}) := F_v\dot{q} + F_s \operatorname{sgn}(\dot{q})$ . Joint PI controllers have been used as servo controllers. Because of the existence of the abrupt changes resulting from the impacts in the hybrid model, the servo controller does not include the derivative terms. We have designed  $P_H = 30$ ,  $P_K = 30$ ,  $I_H = 10$  and  $I_K = 10$  for the servo controllers at the hip and the knee joints. Also in optimization problem, we tune  $D_m = 10$  (m) and  $t_f = 10$  (s). By using Genetic algorithm, the optimal solution of the optimization problem in (37) is determined after 115 generations. The optimal solution of the optimization problem in (37) is equal to  $X = (-0.063, 0.429, 0.172, 0.141, -0.109, -0.016)^T$ .

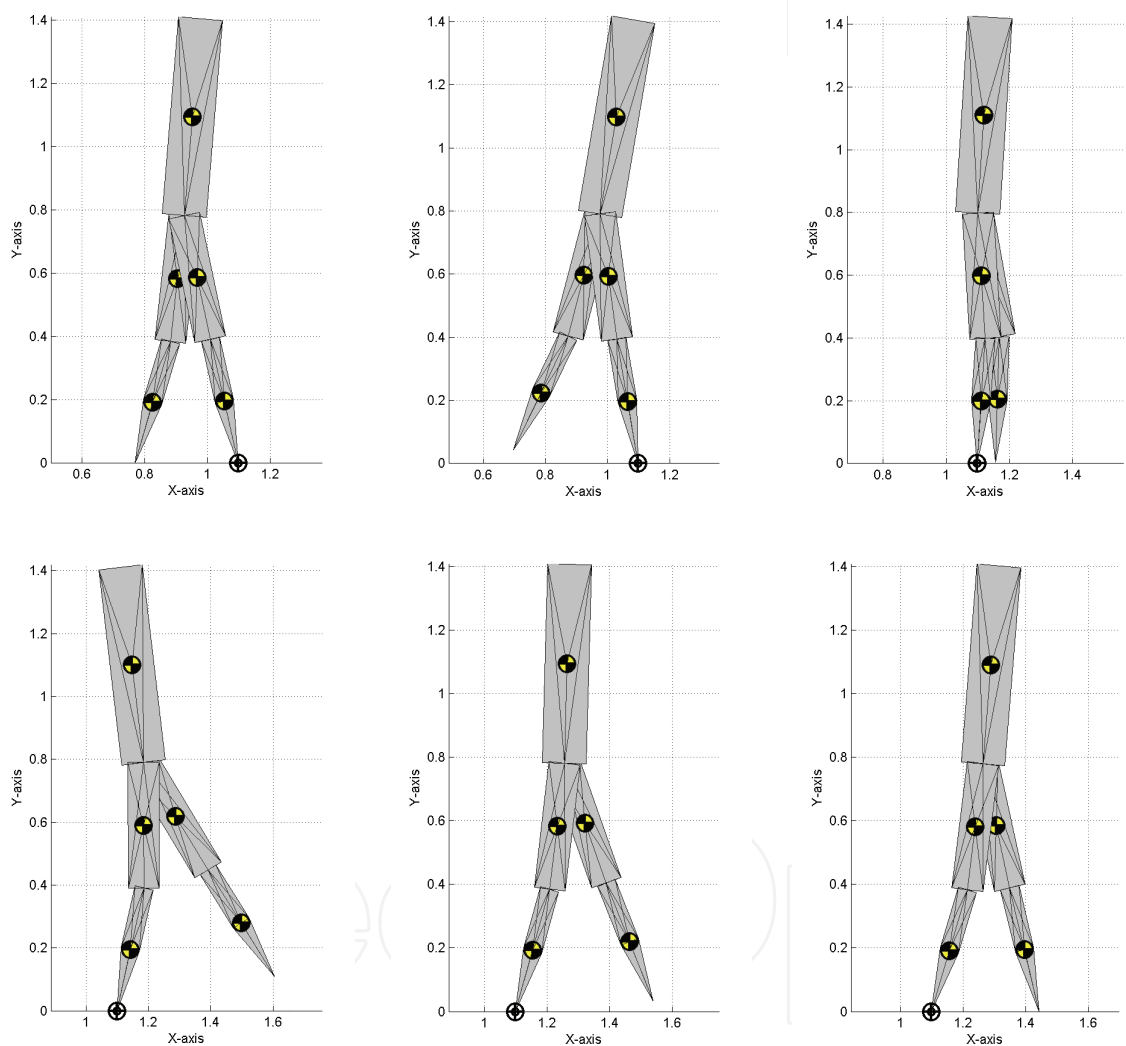


Fig. 5. The snapshots of one step for the biped robot with the best fitness.

The period of the neural oscillators in the biped robot with the best fitness is equal to 1.10 (s). The time between consecutive impacts for this robot is equal to  $T = 0.55$  (s). Also the step length during the walking (the distance between consecutive impacts) is equal to  $sl = 0.33$  (m). The snapshots of one step for the best biped robot at limit cycle in this set of experiments are depicted in Fig. 5. In this picture, the left leg is taking a step forward. It can be seen that the swing leg performs a full swing and it allows sufficient ground clearance for



the foot to be transferred to a new location. In Fig. 6, the CPG outputs and the joint angle positions of the leg joints during 10 (s) are shown with dashed lines and solid lines, respectively. Figure 7 depicts the phase plot and the limit cycle of joint angle vs. velocity at the unactuated joint ( $q_0 - \dot{q}_0$  plane) during 10 (s). Also Fig. 8 depicts the limit cycles at the phase plots of the leg joints during 10 (s).

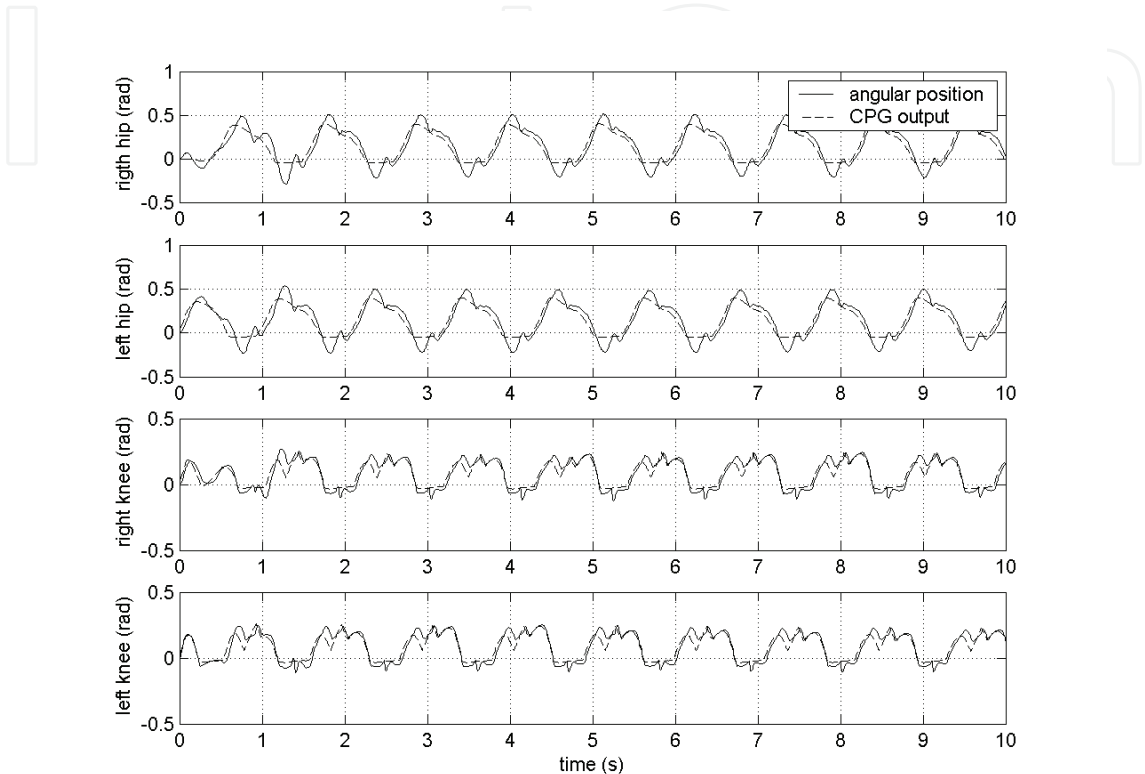


Fig. 6. The CPG outputs and the joint angle positionsof leg joints during 10 (s) .

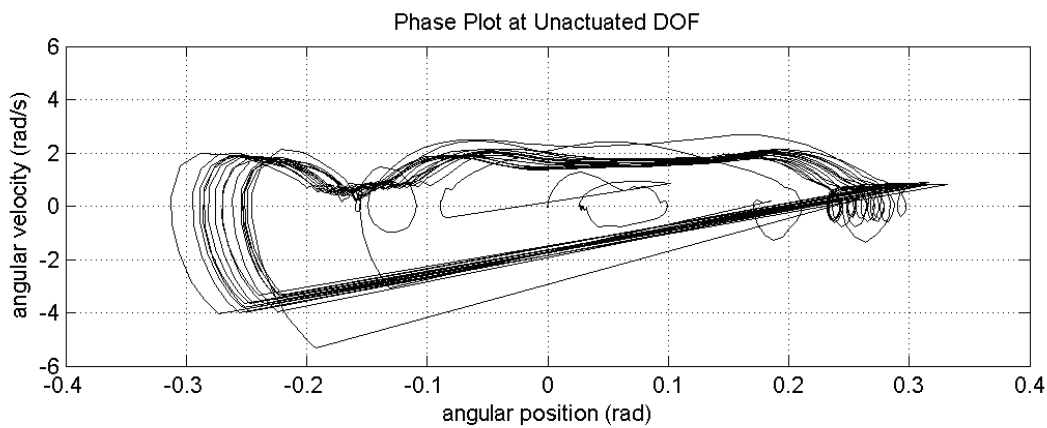


Fig. 7. The phase plot of joint angle vs. velocity at the unactuated joint ( $q_0 - \dot{q}_0$  plane) during 10 (s) .

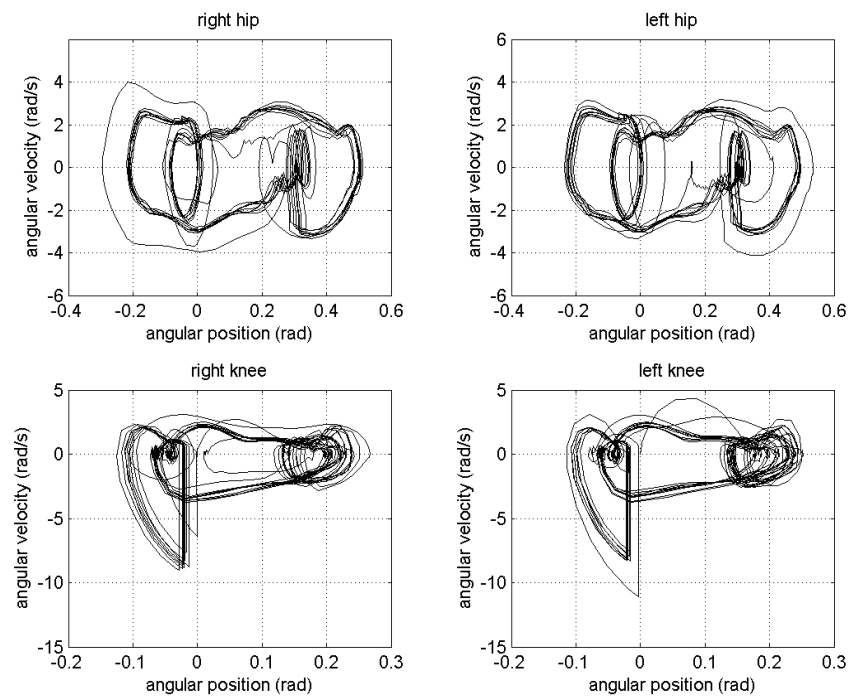


Fig. 8. The phase plots of joint angle vs. velocity at the leg joints during 10 (s) .

Control signals of the servo controllers during 10 (s) are depicted in Fig. 9. The validity of the reduced single support phase model and impact model can be seen by plotting the ground reaction forces as plotted in Fig. 10.

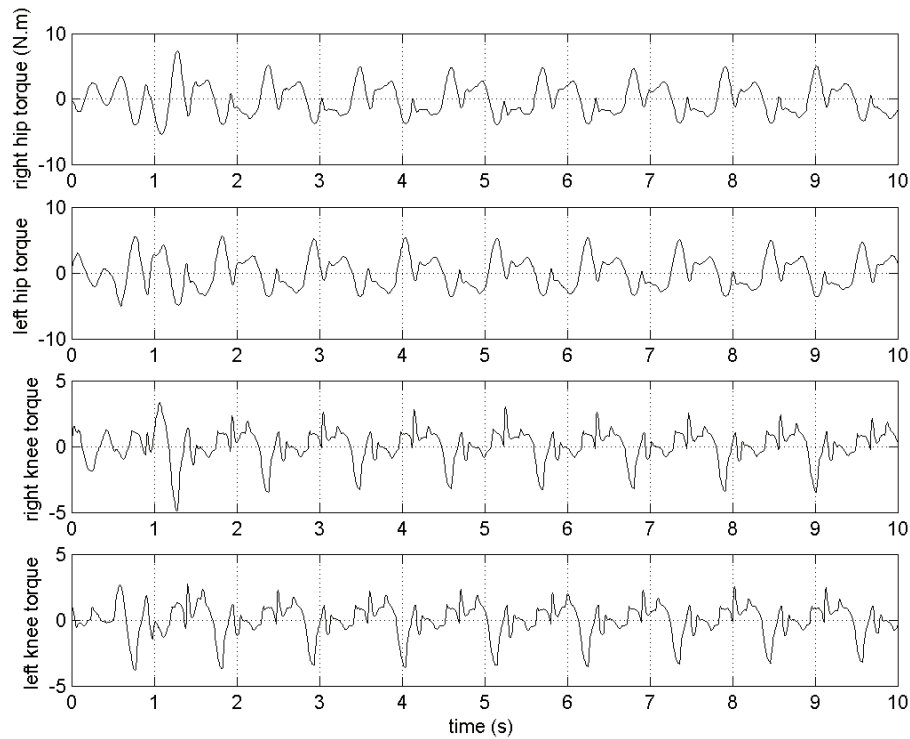


Fig. 9. The control signals of the servo controllers during 10 (s) .

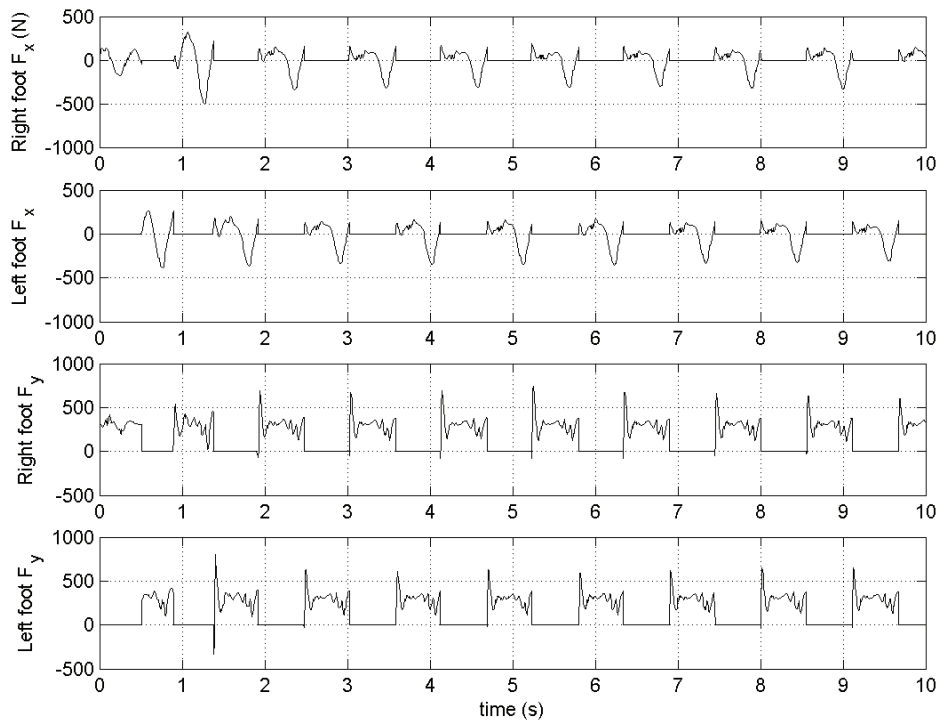


Fig. 10. The ground reaction forces at the leg ends during 10 (s) .

For evaluating the robustness of the limit cycle of the closed loop system, an external force as disturbance is applied to the body of the biped robot. We assume that the external force is applied at the center of mass of the torso and it can be given by  $F_d(t) := F_d(u(t - t_d) - u(t - t_d - \Delta t_d))$  where  $F_d$  is the disturbance amplitude,  $t_d$  is the time when the disturbance is applied,  $\Delta t_d$  is the duration of the pulse and  $u(.)$  is a unit step function. The stick figure of the robot for a pulse with amplitude  $F_d = 25$  (N) and with pulse duration equal to  $\Delta t_d = 0.5$  (s) which is applied at  $t_d = 3$  (s) is shown in Fig. 11. This figure shows the robustness of the limit cycle due to disturbance. Also Fig. 12 shows the stable limit cycle at the unactuated joint. Figure 13 shows the maximum value of the positive and negative pulses vs. pulse duration which don't result in falling down.

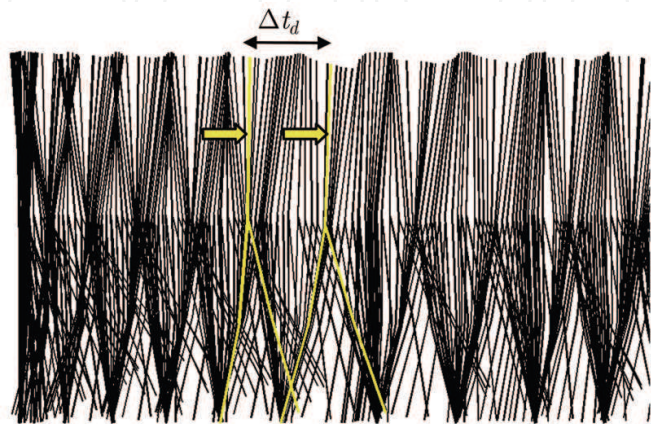


Fig. 11. Stick figure of the robot.

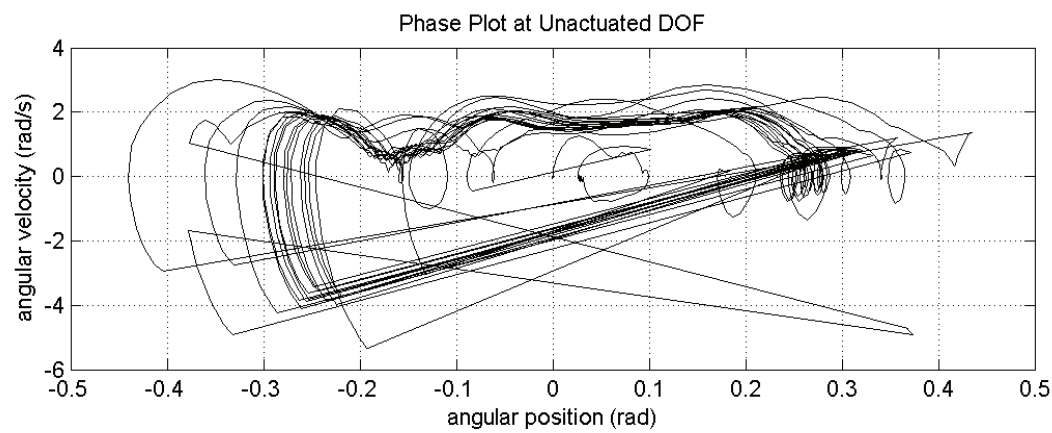


Fig. 12. The phase plot of joint angle vs. velocity at the unactuated joint.

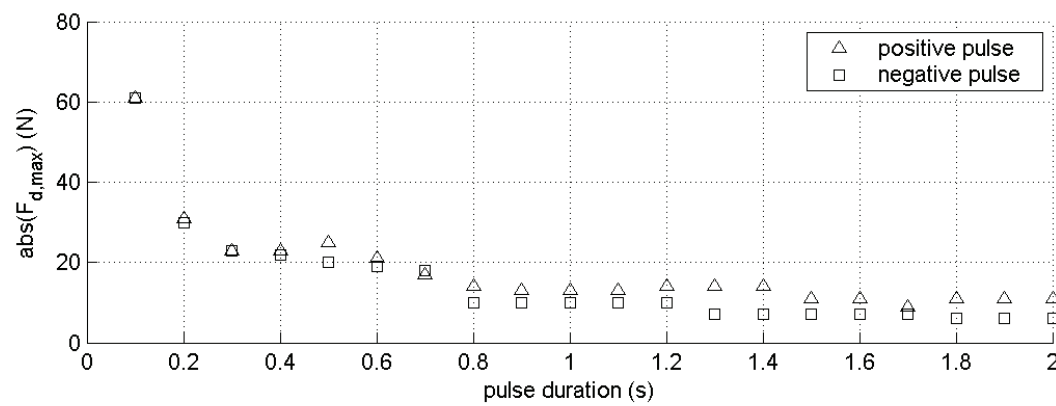


Fig. 13. Maximum amplitude of the pulse vs. pulse duration.

7. Conclusion

In this chapter, the hybrid model was used for modeling the underactuated biped walker. This model consisted of single support phase and the instantaneous impact phase. The double support phase was also assumed to be instantaneous. For controlling the robot in underactuated walking, a CPG network and a new feedback network were used. It is shown that the period of the CPG is the most important factor influencing the stability of the biped walker. Biological experiments show that humans exploit the natural frequencies of their arms, swinging pendulums at comfortable frequencies equal to the natural frequencies. Extracting and using the natural frequency of the links of the robots is a desirable property of the robot controller. According to this fact, we match the endogenous frequency of each neural oscillator with the resonant frequency of the corresponding link. In this way, swinging motion or supporting motion of legs is closer to free motion of the pendulum or the inverted pendulum in each case and the motion is more effective. It is well known in biology that the CPG network with feedback signals from body can coordinate the members of the body, but there is not yet a suitable biological model for feedback network. In this chapter, we use tonic stretch reflex model as the feedback signal at

the hip joints of the biped walker as studied before. But one of the most important factors in control of walking is the coordination or phase difference between the knee and the hip joints in each leg. We overcome this difficulty by introducing a new feedback structure for the knee joints oscillators. This new feedback structure forces the mechanical system to fix the stance knee at a constant value during the single support phase. Also, it forces the swing knee oscillator to increase its output at the beginning of swinging phase and to decrease its output at the end of swinging phase.

The coordination of the links of the biped robot is done by the weights of the connections in the CPG network. For tuning the synaptic weight matrix in CPG network, we define the control problem of the biped walker as an optimization problem. The total cost function in this problem is defined as a summation of the sub cost functions where each of them evaluates different criterions of walking such as distance travelled by the biped robot in the sagittal plane, the height of the CoM and the regulation of the angular momentum about the CoM. By using Genetic algorithm, this problem is solved and the synaptic weight matrix in CPG network for the biped walker with the best fitness is determined. Simulation results show that such a control loop can produce a stable and robust limit cycle in walking of the biped walker. Also these results show the ability of the proposed feedback network in correction of the CPG outputs. This chapter also shows that by using the resonant frequencies of the links, the number of unknown parameters in the CPG network is reduced and hence applying Genetic algorithm is easier.

## 8. References

- [1] J. W. Grizzle, C. Moog, and C. Chevallereau, "Nonlinear control of mechanical systems with an unactuated cyclic variable," *IEEE Transactions on Automatic Control*, vol. 30, no. 5, pp. 559-576, May 2005.
- [2] Y. Hurmuzlu, F. Genot, and B. Brogliato, "Modeling, stability and control of biped robots-a general framework," *Automatica*, vol. 40, pp. 1647-1664, 2004.
- [3] C. Chevallereau, G. Abba, Y. Aoustin, F. Plestan, E.R. Westervelt, C. Canduas-de Wit, and J. W. Grizzle, "RABBIT: A testbed for advanced control theory," *IEEE Control Systems Magazine*, vol. 23, no. 5, pp. 57-79, October 2003.
- [4] M. Vukobratovic and D. Juricic, "Contribution on the synthesis of biped gait," *IEEE Transactions on Biomedical Engineering*, vol. 16, no.1, pp. 1-6, 1969.
- [5] A. Takanishi, M. Ishida, Y. Yamazaki, and I. Kato, "The realization of dynamic walking robot WL-10RD," *Int. Conf. Advanced Robotics*, 1985, pp. 459-466.
- [6] C. L. Shin, Y. Z. Li, S. Churng, T. T. Lee, and W. A. Cruver, "Trajectory synthesis and physical admissibility for a biped robot during the single support phase," *IEEE Int. Conf. Robotics and Automation*, 1990, pp. 1646-1652.
- [7] K. Hirai, M. Hirose, Y. Haikawa, and T. Takenaka, "The development of honda humanoid robot," *IEEE Int. Conf. Robotics and Automation*, 1998, pp. 1321-1326.
- [8] A. Dasgupta and Y. Nakamura, "Making feasible walking motion of humanoid robots from human motion capture data," *IEEE Int. Conf. Robotics and Automation*, 1999, pp. 1044-1049.
- [9] A. Goswami, "Postural stability of biped robots and the foot rotation indicator (FRI) point," *International Journal of Robotic Research*, vol. 18, no. 6, pp. 523-533, June 1999.

- [10] F. Plestan, J. W. Grizzle, E. R. Westervelt, and G. Abba, "Stable walking of a 7-DOF biped robot," *IEEE Transactions on Robotics and Automation*, vol. 19, no. 4, pp. 653-668, August 2003.
- [11] T. McGeer, "Passive dynamic walking," *International Journal of Robotic Research*, vol. 9, no. 2, pp. 62-82, 1990.
- [12] E. R. Westervelt, J. W. Grizzle, and D. E. Koditschek, "Hybrid zero dynamics of planar biped walkers," *IEEE Transactions on Automatic Control*, vol. 48, no. 1, pp. 42-56, January 2003.
- [13] A. Isidori, *Nonlinear Control Systems: An Introduction*, 3rd ed. Berlin, Germany: Springer-Verlag, 1995.
- [14] A. Isidori and C. Moog, "On the nonlinear equivalent of the notion of transmission zeros," in *Proc. IIASA Conf.: Modeling Adaptive Control*, C. Byrnes and A. Kurzhanski, Eds., Berlin, Germany, 1988, pp. 146-157.
- [15] J. Guckenheimer and P. Holmes, *Nonlinear Oscillations, Dynamical Systems, and Bifurcations of Vector Fields*, corrected second printing ed., ser. Applied Mathematical Sciences. New York: Springer-Verlag, 1996, vol. 42.
- [16] B. Morris and J. W. Grizzle, "A restricted Poincaré map for determining exponentially stable periodic orbits in systems with impulse effects: Application to bipedal robots," in *Proc. of IEEE 2005 Conference on Decision and Control*, 2005.
- [17] S. Nersesov, V. Chellaboina, and W. Haddad, "A generalized of Poincaré's theorem to hybrid and impulsive dynamical systems," *Int. J. Hybrid Systems*, vol. 2, pp. 35-51, 2002.
- [18] Y. Hurmuzlu, "Dynamics of bipedal gait - part 2: stability analysis of a planar five-link biped," *Journal of Applied Mechanics*, vol. 60, pp. 337-343, June 1993.
- [19] J. H. Choi and J. W. Grizzle, "Feedback control of an underactuated planar bipedal robot with impulsive foot action," *Robotica*, vol. 23, pp. 567-580, September 2005.
- [20] J. E. Pratt and R. Tedrake, "Velocity based stability margins for fast bipedal walking," <http://www.ai.mit.edu/projects/leglab>, 2007.
- [21] S. Grillner, "Control of locomotion in bipeds, tetrapods and fish," *Handbook of Physiology II*, American Physiol. Society, Bethesda, MD, pp. 1179-1236, 1981.
- [22] G. Taga, Y. Yamaguchi, and H. Shimizu, "Self-organized control of bipedal locomotion by neural oscillators," *Biolog. Cybern.*, vol. 65, pp. 147-159, 1991.
- [23] G. Taga, "A model of the neuro-musculo-skeletal system for human locomotion II: real-time adaptability under various constraints," *Biolog. Cybern.*, vol. 73, pp. 113-121, 1995.
- [24] K. Matsuoka, "Mechanism of frequency and pattern control in the neural rhythm generators," *Biolog. Cybern.*, vol. 56, pp. 345-353, 1987.
- [25] K. Matsuoka, "Sustained oscillations generated by mutually inhibiting neurons with adaptation," *Biolog. Cybern.*, vol. 52, pp. 367-376, 1985.
- [26] M. M. Williamson, "Neural control of rhythmic arm movements," *Neural Networks*, vol. 11, pp. 1379-1394, 1998.
- [27] S. Miyakoshi, G. Taga, Y. Kuniyoshi, and A. Nagakubo, "Three dimensional bipedal stepping motion using neural oscillators-towards humanoid motion in the real word," *IROS98*, pp. 84-89, 1998.



- [28] H. Kimura, Y. Fukuoka, Y. Hada, and K. Takase, "Three-dimensional adaptive dynamic walking of a quadruped rolling motion feedback to CPGs controlling pitching motion," *IEEE International Conference on Robotics and Automation*, 2002, pp. 2228-2233.
- [29] H. Kimura and Y. Fukuoka, "Adaptive dynamic walking of the quadruped on irregular terrain –autonomous adaptation using neural system model," *IEEE International Conference on Robotics and Automation*, 2000, pp. 436-443.
- [30] H. Ye, A. N. Michel, and L. Hou, "Stability theory for hybrid dynamical systems," *IEEE Trans. Automatic Control*, vol. 43, no. 4, pp. 461-474, Apr. 1998.
- [31] B. Brogliato, "Some perspectives on the analysis and control of complementarity systems," *IEEE Transaction on Automatic Control*, vol. 48, no. 6, pp. 918-935, 2003.
- [32] B. Brogliato, S. I. Niculescu, and M. Monteiro, "On the tracking control of a class of complementarity-slackness hybrid mechanical systems," *Systems and Control Letters*, vol. 39, pp. 255-266, 2000
- [33] B. Brogliato, S. I. Niculescu, and P. Orhant, "On the control of finite dimensional mechanical systems with unilateral constraints," *IEEE Transactions on Automatic Control*, vol. 42, no. 2, pp. 200-215, 1997.
- [34] H. Goldstein, *Classic Mechanics*, 2nd ed. Reading, MA: Addison Wesley, 1980.
- [35] M. W. Spong and M. Vidyasagar, *Robot Dynamics and Control*, New York: Wiley, 1991.
- [36] E. Dombre and W. Khalil, *Modeling, Identification and Control of Robots*, Paris: Hermes Sciences, 2002.
- [37] R. M. Murray, Z. Li, and S. Sastry, *A Mathematical Introduction to Robotic Manipulation*, Boca Raton, FL: CRC Press, 1993.
- [38] E. R. Westervelt and J. W. Grizzle, "Design of asymptotically stable walking for a 5-link planar biped walker via optimization," *2002 IEEE International Conference on Robotics and Automation, Wahington D.C.*, 2002, pp. 3117-3122.
- [39] Y. Hurmuzlu, "Dynamics of bipedal gait-part I: objective functions and the contact event of a planar five-link biped," *Journal of Applied Mechanics*, vol. 60, pp. 331-336, June 1993.
- [40] J. H. Choi and J. W. Grizzle, "Planar bipedal robot with impulsive foot action," *IEEE Conf. on Decision and Control*, Paradise Island, Bahamas, December 2004, pp. 296-302.
- [41] Y. Hurmuzlu and D. Marghitu, "Rigid body collisions of planar kinematic chains with multiple contact points," *International Journal of Robotics Research*, vol. 13, no. 1, pp. 82-92, 1994.
- [42] K. Schneider, R. F. Zernicke, R. A. Schmidt and T. J. Hart, "Changes in limb dynamics during the practice of rapid arm movements," *Journal of Biomechanics*, vol. 22, pp. 805-817, 1989.
- [43] G. P. Bingham, R. C. Shmidt, and L. D. Rosenblum, "Hefting for a maximum distance throw: a smart perceptual mechanism," *Journal of Experimental Psychology: Human Perception and Performance*, vol. 15, no.3, pp. 507-528, 1989.
- [44] H. Kimura, Y. Fukuoka, K. Konaga, Y. Hada, and K. Takase, "Towards 3D adaptive dynamic walking of a quadruped robot on irregular terrain by using neural system



- model," *IEEE/RSJ International Conference on Intelligent Robots and Systems*, 2001, pp. 2312-2317.
- [45] M. Abdullah and A. Goswami, "A biomechanically motivated two-phase strategy for biped upright balance control," *IEEE International Conference on Robotics and Automation*, 2005.

IntechOpen

IntechOpen



## Human-Robot Interaction

Edited by Daisuke Chugo

ISBN 978-953-307-051-3

Hard cover, 288 pages

**Publisher** InTech

**Published online** 01, February, 2010

**Published in print edition** February, 2010

Human-robot interaction (HRI) is the study of interactions between people (users) and robots. HRI is multidisciplinary with contributions from the fields of human-computer interaction, artificial intelligence, robotics, speech recognition, and social sciences (psychology, cognitive science, anthropology, and human factors). There has been a great deal of work done in the area of human-robot interaction to understand how a human interacts with a computer. However, there has been very little work done in understanding how people interact with robots. For robots becoming our friends, these studies will be required more and more.

### How to reference

In order to correctly reference this scholarly work, feel free to copy and paste the following:

Nasser Sadati, Guy A. Dumont, and Kaveh Akbari Hamed (2010). Design of a Neural Controller for Walking of a 5-Link Planar Biped Robot via Optimization, Human-Robot Interaction, Daisuke Chugo (Ed.), ISBN: 978-953-307-051-3, InTech, Available from: <http://www.intechopen.com/books/human-robot-interaction/design-of-a-neural-controller-for-walking-of-a-5-link-planar-biped-robot-via-optimization>

**INTECH**  
open science | open minds

### InTech Europe

University Campus STeP Ri  
Slavka Krautzeka 83/A  
51000 Rijeka, Croatia  
Phone: +385 (51) 770 447  
Fax: +385 (51) 686 166  
[www.intechopen.com](http://www.intechopen.com)

### InTech China

Unit 405, Office Block, Hotel Equatorial Shanghai  
No.65, Yan An Road (West), Shanghai, 200040, China  
中国上海市延安西路65号上海国际贵都大饭店办公楼405单元  
Phone: +86-21-62489820  
Fax: +86-21-62489821

© 2010 The Author(s). Licensee IntechOpen. This chapter is distributed under the terms of the [Creative Commons Attribution-NonCommercial-ShareAlike-3.0 License](https://creativecommons.org/licenses/by-nc-sa/3.0/), which permits use, distribution and reproduction for non-commercial purposes, provided the original is properly cited and derivative works building on this content are distributed under the same license.

IntechOpen

IntechOpen